Sparse Reconstruction of RF Tomography with Dynamic Dictionary

Jia Li[1], Robert L. Ewing[2], Charles A. Berdanier[2], Daniel Wetzel[2], and Xiaoping Shen[3]

[1]Department of Electrical and Computer Engineering, Oakland University, Rochester, MI 48309
[2]Sensors Directorate, Air Force Research Lab, WPAFB, OH 45433
[3]Department of Mathematics, Ohio University, Athens, OH 45701

***Abstract*—In this paper, we explore sparse reconstruction of RF tomography with sensors pseudo randomly distributed on a ring. Multilevel scattering and multipath propagation are considered in the system model. A novel approach of dynamically building dictionary for reconstruction is proposed. Under the assumption of sparse target, the proposed method can significantly reduce the size of dictionary and computational complexity of reconstruction. Numerical simulation shows that the method is effective in removing ghost targets caused by multipath propagation, and is fairly accurate in estimating target reflectivity.**

***Index Terms*—RF tomography, sparse reconstruction, dynamic dictionary, ghost target, multipath propagation**

I. Introduction

Radio frequency (RF) tomography has attracted lots of research interests in the past decade due to its potential in defense, homeland security and commercial applications [1]–[3]. Generally speaking, RF tomography is an inverse scattering problem, and has similarity to computed tomography in medical domain [4]. The imaging mechanism is to illuminate the region of interest (ROI) using RF waveforms, and infer the dielectric properties of ROI from the scattered waveforms recorded. When a RF waveform propagates from transmitter to receiver, it may be scattered multiple times and reach the receiver through different paths. The propagation paths are usually determined by the number of scatterers and their locations in ROI. This is the well-known multipath propagation phenomenon in RF imaging.

As most of the inverse problems, RF tomography is an optimization problem, which objective function is determined by system model and metric used. For RF imaging system, multipath propagation can be modeled by including multiple level of scattering in the system model. For example, Leigsnering, etc has investigated multipath propagation in through-the-wall radar imaging [5], [6]. The reflections from surrounding walls are modeled using prior knowledge of the location and thickness of walls. In [7], ghost images caused by multipath propagation has been exploited in radar target classification. In both studies, the locations of higher order scatterers are assumed to be known so the system model is predetermined and fixed throughout the reconstruction process.

In this paper, we consider to reconstruct 2D tomography of point targets in free space. Each target is not only a first order scatterer, but also higher order scatterer on the propagation paths of waveforms reflected from other targets. As the number of targets and their locations are unknown, a naive approach to model multipath propagation is to include every pixel of tomography as both first order scatterer and higher order scatterer in the system model. However, such an exhaustive approach can cause the size of reconstruction dictionary grow exponentially with the image size and lead to significant increase in computational complexity of reconstruction. To maintain the computational cost at a practical level, we propose to exploit the sparsity of targets and dynamically build the dictionary of reconstruction. In each iteration, the phrases corresponding to zero reflectivity are removed from, and the phrases corresponding to the next order of scattering are added to the dictionary. The results show that the proposed algorithm can effectively remove ghost targets caused by multipath propagation and greatly reduce the computational cost.

In Section II, multipath propagation and the formation of ghost targets are illustrated through an example. The system model of RF tomography based on multipath propagation is derived. In Section III, we discuss how the sparsity of targets can be exploited to dynamically build the dictionary of system model. After that, the results of numerical simulations are presented in Section IV. We conclude the paper and discuss future work in Section V.

II. System Model

RF imaging system is usually composed of distributed RF sensors to achieve spatial and frequency diversity. The sensors can be inhomogeneous transmitters and receivers, or homogeneous transceivers with monostatic or multistatic setup. In the derivation following, we assume stationary point target, isotropic reflection, multistatic system and free space propagation.

Let M be the number of RF sensors and N be the number of pixels. Assume sensors are randomly located outside of the region of interest. Let σ_i represent the reflectivity of the i-th pixel, $i = 1 \dots N$. When only considering the waveform reflected from point targets directly, i.e. there is no secondary or higher order scatterers, the received signal is a combination of all the directly reflected waveforms,

$$r_{mm'}(t) = \sum_{i=1}^{N} \sigma_i p(t - \tau_{mm'}(i)) e^{-j2\pi f \tau_{mm'}(i)}, \quad (1)$$

where m and m' are the indices of transmitter and receiver, separately, σ_i is the reflectivity of the i-th pixel, $\tau_{mm'}(i)$ is the bistatic propagation delay from the m-th transmitter to the i-th pixel, and back to the m'-th receiver. Please note the waveform propagated through direct path is not included in Eq. (1) because it is usually removed in preprocessing step.

When there are multiple targets in the ROI, a transmitted pulse can propagate through different paths and experience multilevel scattering before reaching the receiver. We discuss the formation of ghost targets and the model of multipath propagation in the following section.

A. Multipath propagation

Multipath propagation is a major challenge in RF imaging. For stationary targets, echoes from multiple paths can easily confuse the receiver and cause the formation of "ghost targets" in reconstructed image. Fig. 1 illustrates how multipath propagation leads to a ghost target in the case of two point targets in a ROI. It's well known that target location can be calculated through the intersection of ellipses in bistatic setup, where ellipses are determined by the transmitter and receiver location, as well as the propagation delay experienced by the echo. In Fig. 1, there are two point targets. The red lines represent the paths of the first order reflection from target 1, i.e. the waveform travels from transmitter (Tx) to target 1, then to receiver 1 (Rx1) and receiver 2 (Rx2), separately. The two ellipses drawn by solid lines are determined by the two bistatic pairs (Tx, Rx1), (Tx, Rx2) and the corresponding propagation delays. We denote the two ellipses as e_1 and e_2, separately. The intersection of e_1 and e_2 inside the ROI is the location of target 1. The blue line indicates the propagation path when the echo reflected from target 1 is further reflected by target 2, then reaches receiver 1. The delay of this secondary scattering propagation path and the location of bistatic pair (Tx, Rx1) form another ellipse, e_3, which is drawn in dashed line. If the system model only considers the first order scatterers, the intersection of e_2 and e_3 will appear in the reconstruct image as a ghost target. Generally speaking, each target in the field of view can serve as higher order scatterers on the propagation paths of the echoes reflected from other targets. The intersections of all the ellipse pairs will lead to many ghost targets in reconstruction. To distinguish ghost targets from true targets, Eq. (1) is modified to include multilevel scatterers and multipath propagation in system model,

$$r_{mm'}(t) = \sum_{i=1}^{N} \sum_{j=1}^{K_i} \sigma_{ij} p(t - \tau_{mm',ij}) e^{-j2\pi f \tau_{mm',ij}}, \quad (2)$$

where K_i is the total number of paths that have i-th pixel as the first order scatterer, j is the index of paths, σ_{ij} is the

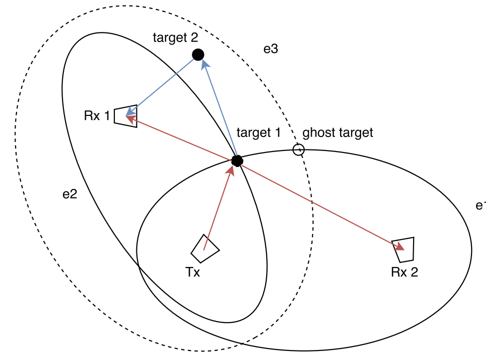

Figure 1: Multipath propagation and ghost target.

attenuation coefficient of the path, $p(t)$ is the baseband pulse transmitted and $\tau_{mm',ij}$ is the propagation delay of the path.

The above multipath model can be discretized by sampling the echo propagated along each path and the received waveform. The attenuation coefficients can be stacked into a $NK_i \times 1$ vector. This will lead to a discrete model,

$$\boldsymbol{r} = \boldsymbol{P}\boldsymbol{\sigma} \quad (3)$$

where $\boldsymbol{r}$ is a column vector representing the sampled received waveform, $\boldsymbol{P}$ is a matrix which columns are delayed version of pulses along each path, and $\boldsymbol{\sigma}$ is the column vector of attenuation coefficients. $\boldsymbol{P}$ is also called dictionary or forward model of the bistatic pair (m, m'). It can be pre-calculated for each pair of sensors in the imaging system. The reconstruction is an inverse problem, which estimates the unknown vector $\boldsymbol{\sigma}$ from the noisy observation $\boldsymbol{r}$.

For this multipath model, if we only consider the first and secondary scatterers, the total number of paths is N^2 for an image of N pixels. The size of $\boldsymbol{P}$ will be $L \times N^2$, where L is the length of $\boldsymbol{r}$. Such a huge dictionary will make the computational cost of reconstruction too burdensome. In the next section, we propose to exploit the sparsity of targets to build the dictionary dynamically.

III. Sparse Reconstruction

Sparse representation and reconstruction have been widely studied to efficiently sample and reconstruct sparse signals [8]–[10]. It concerns solving optimization problems of the form,

$$\min_{\boldsymbol{x} \in \mathbb{R}^n} \frac{1}{2} ||\boldsymbol{y} - \boldsymbol{A}\boldsymbol{x}||_2^2 + \lambda ||\boldsymbol{x}||_1, \quad (4)$$

where $\boldsymbol{y} \in \mathbb{R}^k$, $\boldsymbol{A} \in \mathbb{R}^{k \times n}$, $\lambda > 0$, $|| \cdot ||_2$ and $|| \cdot ||_1$ stand for l_2 norm and l_1 norm, separately. As k is usually less than n, dictionary $\boldsymbol{A}$ is overcomplete or the system is under-determined, i.e. there are infinite number of solutions to the problem of $\boldsymbol{y} = \boldsymbol{A}\boldsymbol{x}$. The l_1 regularizer is imposed to reduce the space of solutions, and identify a sparse solution to the problem.

For RF tomography, if the number of targets is much smaller than the number of pixels, the attenuation vector $\boldsymbol{\sigma}$ is sparse. So Eq. (3) can be solved through sparse reconstruction. However, as aforementioned, the overcomplete dictionary $\boldsymbol{P}$ is too large for efficient computation. We propose to dynamically construct dictionary $\boldsymbol{P}$ to reduce the size of dictionary and computational cost.

A. Dynamic dictionary

An efficient dictionary is important in sparse representation and reconstruction. Although different dictionary learning rules have been developed for different applications, the problem is generally formulated as

$$\min_{\boldsymbol{A},\boldsymbol{x}} \frac{1}{2}||\boldsymbol{y} - \boldsymbol{A}\boldsymbol{x}||_2^2 + \lambda||\boldsymbol{x}||_1. \tag{5}$$

In [11], sparse reconstruction with dynamic dictionary was studied for parameter estimation from noisy signals. For our application, each phrase in dictionary $\boldsymbol{P}$ is a delayed version of pulse $p(t)$. The delay is determined by the length of the corresponding propagation path. For computational efficiency, we propose to iteratively prune the dictionary and introduce new propagation paths. We initialize the dictionary with echoes directly reflected from all N pixels. After the first reconstruction, $\hat{\boldsymbol{\sigma}}_1$ contains nonzero values at target and ghost target locations. Based on the information of $\hat{\boldsymbol{\sigma}}_1$, all the phrases corresponding to zero values in $\hat{\boldsymbol{\sigma}}_1$ are removed from $\boldsymbol{P}$. New phrases corresponding to the paths with first and secondary scatterers are appended to $\boldsymbol{P}$. Please note only pixels with nonzero values in $\hat{\boldsymbol{\sigma}}_1$ are considered as the secondary scatterers, which is significant less than the original N pixels. The total number of phrases in a dynamic dictionary is determined by the number of targets, the number of bistatic imaging pairs, and the order of scatterers considered. With more paths corresponding to higher order scattering included in dictionary $\boldsymbol{P}$, ghost targets are either removed or suppressed. The pseudo code of the reconstruction algorithm is given in Algorithm 1. In the output $\hat{\boldsymbol{\sigma}}$, nonzero values associated with the paths of first order scattering are kept as the reflectivity of targets.

Algorithm 1 Sparse Reconstruction of RF Tomography with Dynamic Dictionary

```
procedure SPARSE RECONSTRUCTION
    Input: r
    Initializatioin: P_1 = [p_1, p_2, ..., p_N]
    for i = 1 to Highest order of scattering do
        σ̂_i = arg min_σ (1/2)||r − P_i σ||_2^2 + λ||σ||_1
        P_{i+1} = P_i − {p_j | σ̂_ij = 0}
        P_{i+1} = P_{i+1} ∪ {p | pulses along paths with
                (i+1)-th order scattering }
    end for
    Output: Reflectivity of the first order scatterers.
end procedure
```

IV. NUMERICAL SIMULATIONS

In this section, we present numerical simulation and results obtained using the reconstruction method proposed above. A two dimensional radio frequency imaging system is simulated. As illustrated in Fig. 2, homogeneous RF sensors are pseudo randomly distributed on a ring of 80m radius. Each sensor is a transceiver that can transmit and receive arbitrary waveforms in the frequency range of 200M-2G Hz. The dielectric property of the area inside of the ring is to be estimated through RF tomography reconstruction. The image is a uniform 50×50 grid centered at the origin of the ring. The pixel resolution is 2m by 2m, which is chosen according to the bandwidth of simulated pulse.

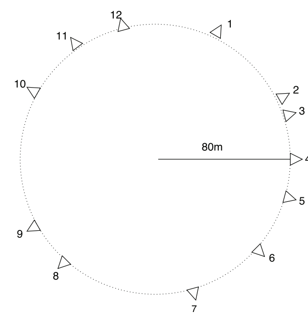

Figure 2: Setup of RF sensors.

The simulated pulse is a linear frequency modulated chirp with 40M Hz bandwidth. The simulation of multipath propagation includes direct path, and the paths containing first and secondary scattering. The received waveform $\boldsymbol{r}$ is a linear combination of waveforms propagated along different paths. The built-in MATLAB function lasso() has been used for iterative sparse reconstruction. The value of λ is manually assigned to be 1 to achieve the desired level of sparsity. The fusion of multiple bistatic pairs is realized by stacking the dictionary of all imaging pairs into one matrix.

A. Noiseless case

In our experiment, we first simulated noiseless received waveform for the scenario of 3 targets and 5 sensors. Both targets and sensors are pseudo randomly distributed. In Fig. 3 (a), the locations of RF sensors are indicated by red triangles, and targets are the bright spots in the image. As we can see from Fig. 3 (b) and (c), there are quite a few ghost targets in the first order reconstruction, which are completely removed in the second order reconstruction. The true reflectivity vector of the three targets is $\boldsymbol{\sigma} = [1\ 0.8\ 0.64]$. The reconstructed reflectivity of the targets is $\hat{\boldsymbol{\sigma}} = [0.849\ 0.665\ 0.513]$. The ratio of the estimated reflectivity over the true reflectivity of the three targets is about the same. Experiments show that the gap between the estimated reflectivity and the true reflectivity increases with the value of λ, which is expected as larger λ gives more weight to l_1 penalty. Compared to a total of 2500×2500 phrases in a predetermined dictionary, the second order dynamic dictionary for this case has only 144 phrases because there are only 12 nonzero reflectivity coefficients estimated through the first order reconstruction. Please note the number of estimated nonzero reflectivity coefficients is less than the sum of the number of targets and the number of theoretical ghost targets due to the large value of λ chosen.

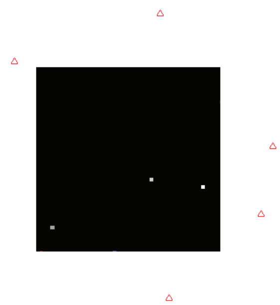

(a) Ground truth

(b) First order reconstruction (c) Second order reconstruction

Figure 3: Noiseless case: 3 targets, 5 sensors.

B. Noisy case

We have also simulated noisy received waveforms for the same scenario at 4 different noise levels. Additive white Gaussian noise were simulated and added to the received waveform. Table I summaries the reconstruction results. The true reflectivity of the three targets is the same as the noiseless case. The location index of the three targets is [159 246 807], which is indicated by red color in the table. The estimated reflectivity of the three targets is also indicated by red color.

Table I: Reconstruction results of noisy case.

SNR (dB)	Location Index of Pixels with Nonzero Reflectivity	Estimated Reflectivity
20.96	[159 246 807]	[0.892 0.707 0.525]
15.00	[90 159 246 807]	[0.03 0.848 0.704 0.526]
9.56	[38 159 246 295 807]	[0.0191 0.9695 0.6594 0.0131 0.4974]
4.54	[105 107 159 246 320 346 807 1601]	[0.1058 0.0231 0.3369 0.3026 0.0288 0.0652 0.2893 0.0687]

As can be seen from the table, the number of pixels with nonzero reflectivity increases with the noise level. This is mainly caused by the noise in received waveform instead of multipath propagation. The estimated reflectivity of noisy pixels is usually much smaller than the estimated reflectivity of the targets. This implies target detection can be implemented through thresholding the pixel values of the reconstructed image.

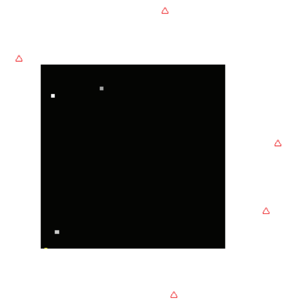

(a) Ground truth

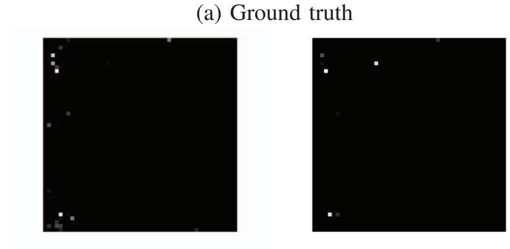

(b) First order reconstruction (c) Second order reconstruction

Figure 4: Noisy case: 3 targets, 5 sensors, SNR = 4.54dB.

Fig. 4 shows the reconstruction results for the case of SNR = 4.54 dB. Compared with the results of noiseless case, the first order reconstruction of noisy case has a lot more nonzero pixels. The second order reconstruction contains 8 nonzero pixels including the 3 target pixels. As the target pixels have larger estimated reflectivity, they appear to be a lot brighter than the noise pixels.

V. Conclusion

We proposed a sparse reconstruction method for RF tomography reconstruction using dynamic dictionary. The dynamically built dictionary can model multipath propagation in RF imaging incrementally, which leads to lower computational cost than predetermined dictionary. Numerical simulations show that the method is effective in removing ghost targets, even in noisy scenarios. Without loss of generality, the same approach can be applied to 3D tomography reconstruction. For future study, we will investigate how dictionary learning can be used to model clutters in a RF imaging environment.

Acknowledgment

This research is supported by National Research Council Research Associateship Program. The authors would also like to thank Air Force Research Lab for the use of its facilities.

References

[1] M. C. Wicks, B. Himed, H. Bascom, and J. Clancy, "Tomography of moving targets (tmt) for security and surveillance," in *Advances in Sensing with Security Applications NATO Security Through Science Series*. Springer, 2006, vol. 2, pp. 323–339.

[2] L. Lo Monte, D. Erricolo, F. Soldovieri, and M. C. Wicks, "Radio frequency tomography for tunnel detection," *IEEE Trans. on Geoscience and Remote Sensing*, vol. 48, no. 3, pp. 1128–1137, 2010.

[3] B. Hamilton, X. Ma, R. Baxley, and S. Matechik, "Propagation modeling for radio frequency tomography in wireless networks," *IEEE Journal of Selected Topics in Signal Processing*, vol. 8, no. 1, pp. 55–65, 2014.

[4] H. D. Griffiths and C. J. Baker, "Fundamentals of tomography and radar," in *Advances in Sensing with Security Applications Series 2*. Springer, 2006, pp. 171–187.

[5] M. Leigsnering, F. Ahmad, M. G. Amin, and A. M. Zoubir, "Specular multipath exploitation for improved velocity estimation in through-the-wall radar imaging," in *Proc. of 2014 IEEE International Conference on Acoustic, Speech and Signal Processing (ICASSP)*, 2014, pp. 1060–1064.

[6] M. Leigsnering, F. Ahmad, M. Amin, and A. Zoubir, "Multipath exploitation in through-the-wall radar imaging using sparse reconstruction," *IEEE Trans. on Aerospace and Electronic Systems*, vol. 50, no. 2, pp. 920–939, April 2014.

[7] G. E. Smith and B. G. Mobasseri, "Analysis and exploitation of multipath ghosts in radar target image classification," *IEEE Trans. on Image Processing*, vol. 23, no. 4, pp. 1581–1592, April 2014.

[8] R. Tibshirani, "Regression shrinkage and selection via the lasso," *Journal of the Royal Statistical Society*, vol. 58, no. 1, pp. 267–288, 1996.

[9] S. S. Chen, D. L. Donoho, and M. A. Saunders, "Atomic decomposition by basis pursuit," *SIAM J. Sci. Comput.*, vol. 20, no. 1, pp. 33–61, 1998.

[10] S. J. Wright, R. D. Nowak, and M. A. T. Figueiredo, "Sparse reconstruction by separable approximation," *IEEE Trans. on Signal Processing*, vol. 57, no. 7, pp. 2479–2493, July 2009.

[11] C. D. Austin, J. N. Ash, and R. L. Moses, "Parameter estimation using sparse reconstruction with dynamic dictionaries," in *Proc. of 2011 IEEE International Conf. on Acoustics, Speech and Signal Processing*, 2011, pp. 2852 – 2855.